International Research Journal of Applied and Basic Sciences
© 2014 Available online at www.irjabs.com
ISSN 2251-838X / Vol, 8 (7): 895-903
Science Explorer Publications

The Effects of External Parallel Direct Current Magnetic Field on a Cold Atmospheric Pressure Argon Plasma Jet

Reza Safari[1]

1. Department of Atomic and Molecular Physics, Faculty of Basic Sciences, University of Mazandaran, Babolsar, Iran

Corresponding Author email: reza8_safari@yahoo.com

ABSTRACT: In this work, external direct current magnetic field effect on the atmospheric pressure plasma jet was investigated, experimentally. The magnetic field was produced using a Helmholtz coil configuration. It was applied parallel to the jet flow. The strength of the magnetic field was 0- 0.28 Tesla between the two coils in parallel application. It was shown that the plasma gas flow plays the main role in magneto-active collision-dominated plasma. The effect of plasma fluid velocity on the jet emission was discussed, qualitatively. It was observed that the external magnetic field has effect on plasma jet in parallel application. The measurements revealed that the plasma jet irradiance increases in parallel field. The former was attributed to increasing plasma number density and in turn shrinks plasma jet number density. As a result, it was concluded that the plasma fluid velocity is responsible for such trends though the magneto-active plasma remains isotropic.
Keywords: Collisional; Isotropic; Magneto Active Plasma; Plasma Fluid Velocity

INTRODUCTION

Recently, much attention has been focused on the atmospheric pressure plasma jet and its applications such as processing technology, engineering, sterilization and treatment such as deposition and etching. In these applications, it is important to identify and study the plasma jet characteristics under various conditions. From this point of view, much experimental and numerical investigation has been carried out to recognize non-thermal plasma jet characteristics (Schutze et al., 1998; Lu et al., 2005; Walsh et al., 2010).

Various types of atmospheric pressure plasma jet with different configurations have been reported, where most of the jets are working with noble gas mixed with a small percentage of reactive gases, such as O_2. Plasma jets that operate with noble gases, can be classified into four categories, i.e. dielectric-free electrode (DFE) jets, dielectric barrier discharge (DBD) jets, DBD-like jets and single electrode (SE) jets that in this research, we applied DBD structure and pure argon gas.

The DBD jet devices can be operated either by kHz ac power or by pulsed dc power. The length of the plasma jet can easily reach several centimeters and depends on gas type and operating voltage. There are several advantages of the non-thermal plasma jets (Lu et al., 2008). First of all, the plasma gas temperature is close to room temperature and second, there is no arcing because of the use of the dielectric barrier. These two characteristics are very important for plasma medicine application, where safety is a strict requirement.

The excitation frequency is important since it influences the behavior of the electrons and the ions. The atmospheric plasma sources can be classified regarding their excitation mode. Three groups are then highlighted: the direct current (DC) and low frequency discharges; the plasmas which are ignited by radio frequency waves and the microwave discharges (Tendero et al., 2006).

In this work, the atmospheric pressure plasma jet was driven by a sinusoidal alternating high voltage power supply 15 kV with very low frequency, 10 kHz. In order to study the plasma characteristics under various conditions, some researchers studied the external magnetic field effects on thermal plasma jet in vacuum chamber because it can be controlled by a strong magnetic field (Koike et al., 2004; Koike and Ono, 2008; Ono et al., 2006; Ono et al., 2007).

The results showed that the thermal plasma jet was constricted by strong magnetic field and several parameters such as number density, temperature and light intensity can be influenced.

In our knowledge, the issue of external magnetic field effect, on non-thermal atmospheric pressure plasma jet has not been studied, yet. In this work, an experimental study was carried out to examine the external direct current magnetic field effects on non-thermal atmospheric pressure plasma jet. Here after,

plasma jet in external magnetic field is named magneto-active atmospheric pressure plasma jet. Optical emission spectroscopy apparatus and imaging technique were utilized to quantify the plasma jet behavior under different conditions.

In recent work, we deal with a collisional magneto-active atmospheric pressure plasma, therefore, the behavior of the transport phenomena seems not to be the same as a typical low pressure magneto-active gas discharge, although the strength of the direct current magnetic field is moderately high.

For a while, look at mobility, conductivity and diffusion tensors in the presence of external magnetic field. These tensors are given by (Krall and Trivelpiece, 1973)

$$\mu = \begin{bmatrix} \mu_\perp & \mu_T & 0 \\ \mu_T & \mu_\perp & 0 \\ 0 & 0 & \mu_\parallel \end{bmatrix}, \quad \sigma = \begin{bmatrix} \sigma_\perp & \sigma_T & 0 \\ \sigma_T & \sigma_\perp & 0 \\ 0 & 0 & \sigma_\parallel \end{bmatrix}, \quad D = \frac{KT}{q}\mu \qquad (1)$$

Where, $\mu_\perp$, μ_T, $\mu_\parallel$ and $\sigma_\perp$, σ_T, $\sigma_\parallel$ are mobility and conductivity tensor elements, respectively. Diffusion tensor D is proportional to mobility tensor. K is Boltzmann's constant, *T* is electron temperature and *q* is the electron charge.

$$\mu_\perp = \frac{q\nu_m}{m\left(\nu_m^2 + \omega_c^2\right)} \qquad \mu_T = \frac{q\omega_c}{m\left(\nu_m^2 + \omega_c^2\right)} \qquad \mu_\parallel = \frac{q}{m\nu_m} \qquad (2)$$

$$\sigma_\perp = \frac{nq^2}{m\left(\nu_m^2 + \omega_c^2\right)} \qquad \sigma_T = \frac{nq^2\omega_c}{m\left(\nu_m^2 + \omega_c^2\right)} \qquad \sigma_\parallel = \frac{nq^2}{m\nu_m} \qquad (3)$$

where, ν_m and ω_c are electron collision frequency for momentum transfer and electron cyclotron angular frequency, respectively. *n* and *m* are the electron number density and mass, respectively. Now, let us examine the magnitude of collision frequency and cyclotron frequency for the electrons in argon plasma.

Without loss of generality, assume the electron temperature in the following estimations to be T_e= 1 ev for both atmospheric and low pressure plasmas. Refer to reference (Raizer, 1997), one can find that for an atmospheric pressure plasma jet, $\nu_m = 4.028\times10^{12} s^{-1}$ and $\omega_c = 7\times10^{10} rad.s^{-1}$ with external direct current magnetic field of B=4000 G. While for a typical low pressure plasma at p=1mTorr, $\nu_m = 5.3\times10^{6} s^{-1}$ and $\omega_c = 7\times10^{10} rad.s^{-1}$ with the same magnetic field strength as before. It is seen that in our case $\left(\omega_c/\nu_m\right)^2 \gg 1$, while in low pressure case, $\left(\omega_c/\nu_m\right)^2 \ll 1$.

This means at atmospheric pressure, when $\left(\omega_c/\nu_m\right)^2 \gg 1$, collisions make the magneto-active collisional plasmas to be isotropic for transport phenomena in which mobility, conductivity and diffusion play roles. Although the applied magnetic field is moderately high, but $\mu_\perp = \mu_\parallel$, $\mu_T \cong 0$. This also holds for conductivity. As a result, the aforementioned tensors lead to be a scalar coefficient for magneto-active atmospheric pressure plasma jet in the presence of external magnetic field.

This characterization indicates that the magneto-active atmospheric pressure plasma jet description is not the same as low pressure magneto-active plasmas. As we treated the atmospheric pressure plasma jet under external magnetic field, we presented analytical models for magneto-active atmospheric pressure plasma jet behavior using MHD fluid equation.

This paper is organized as follows: In section 2, we present the experimental setup and methods, in section 3, we discuss about the experimental results. Discussions and analytical models will be given in section 4. Finally, conclusions will be given in section 5.

EXPERIMENTAL SET UP AND METHODS

Figure 1 shows the experimental setup and methods in this study. The atmospheric pressure plasma jet consists of a tube of Pyrex glass with a length of 35 mm. Powered electrode was set inside the Pyrex tube and grounded ring electrode was attached to the surface of the Pyrex nozzle. The atmospheric pressure plasma jet was driven by a sinusoidal alternating high voltage power supply 15 kV with frequency of 10 kHz.

The plasma was generated at the gas gap between two copper electrodes and exited into the surrounding air outside the nozzle (Fig. 1a). The flow rate of working gas, argon, was 5 lit/min that controlled with mass flow controller. In addition, the jet length was about 20 mm which measured from the nozzle orifice. The maximum width of the jet was 3 mm. Typical V-I characteristics of plasma jet is shown in Fig.2.

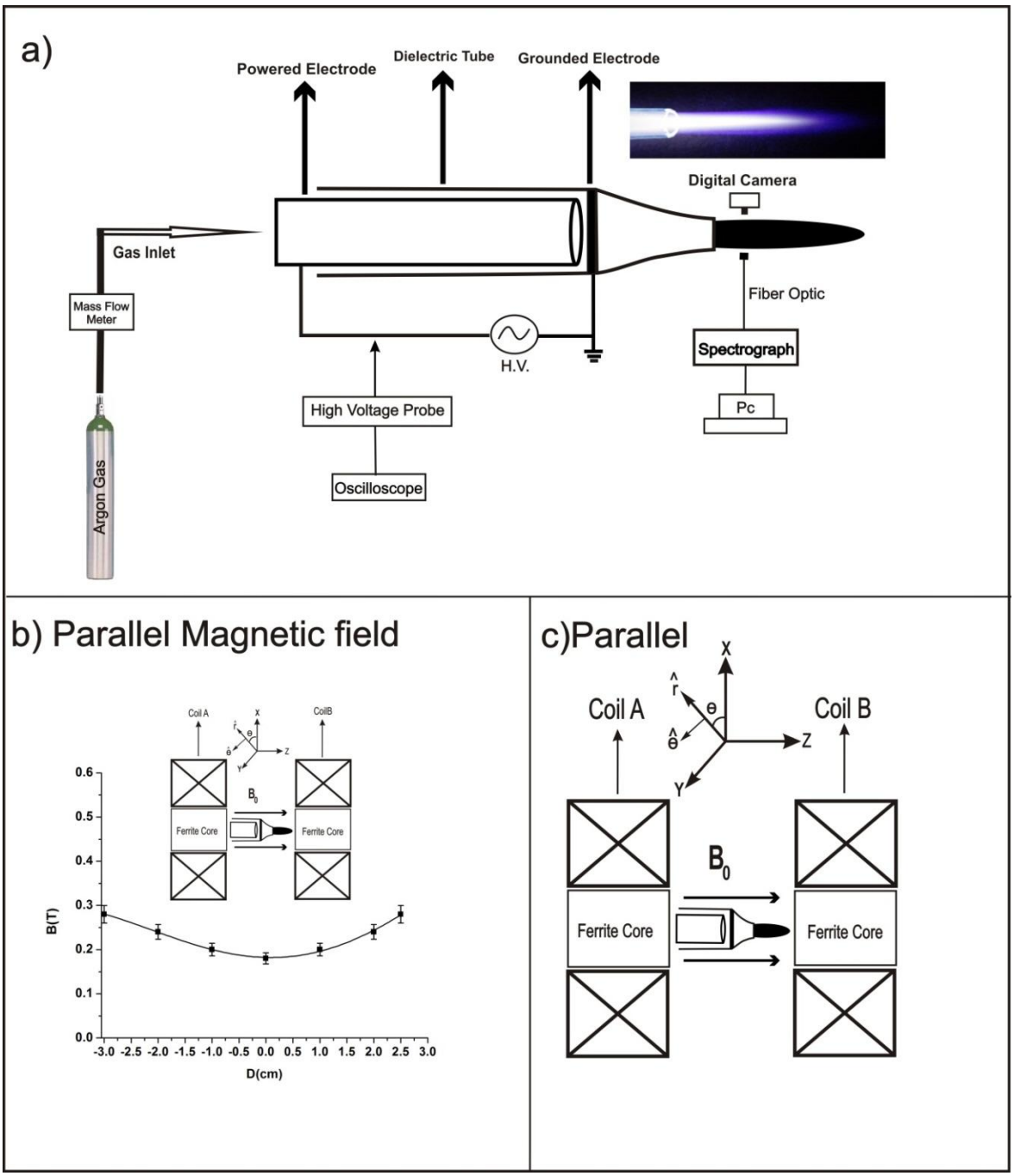

Figure1. (a) Schematic picture of the APPJ set up (b) magnetic field strength in parallel state (c) parallel application of the direct current external magnetic field on the APPJ.

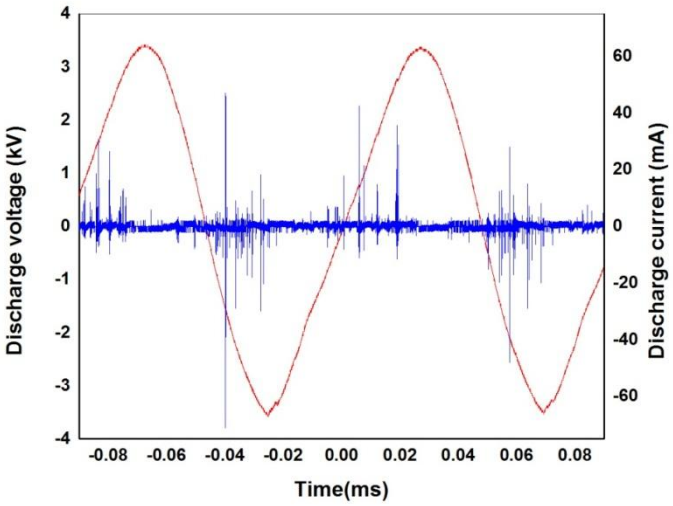

Figure 2. V-I charestirstics of plasma jet

The strength and configurations of the external magnetic field in parallel state were shown in Fig. 1b and Fig. 1c, respectively.

The magnetic field was produced by Helmholtz coil configuration and it was applied parallel and transverse to the jet flow. For deriving the Helmholtz coil, we utilized two direct current power supplies (30 V, 20 A). In order to characterize the Helmholtz coil configurations, numerically, we first estimated the produced magnetic field by flowing current up to 18 A which was supplied by DC power supply(30 V, 20 A). In figure 3, the schematic drawing of each coil is seen.

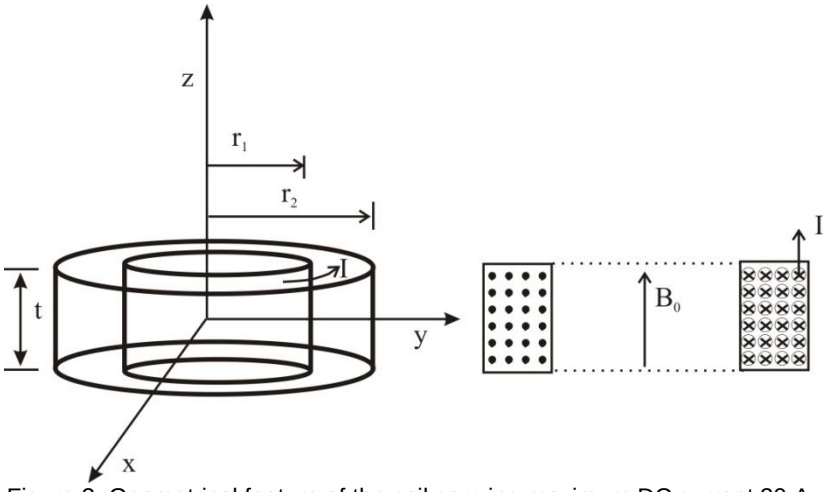

Figure 3. Geometrical feature of the coil carrying maximum DC current 20 A.

Finally, to compute the magnetic field flux on the Helmholtz coil axis, we obtained the following relation for each coil

$$B_z = \frac{\mu_0 NI}{2\delta t}\left(\left(\frac{t}{2}-z\right)Ln\left(r_2+\left(r_2^2+\left(z-\frac{t}{2}\right)^2\right)^{1/2}\right)+\left(\frac{t}{2}+z\right)Ln\left(r_2+\left(r_2^2+\left(z+\frac{t}{2}\right)^2\right)^{1/2}\right)-\left(\frac{t}{2}-z\right)Ln\left(r_1+\left(r_1^2+\left(z-\frac{t}{2}\right)^2\right)^{1/2}\right)-\left(\frac{t}{2}+z\right)Ln\left(r_1+\left(r_1^2+\left(z+\frac{t}{2}\right)^2\right)^{1/2}\right)\right) \quad (4)$$

To make coil, two parallel wires were used, so I is input current of each turn (up to 9 A) while output current of power supply is 18 A. N is the number of turns in each row (40 turns). Number of coil turn is 1600 turns, t is the coil thickness and it was 60 mm, μ_0 is permeability of free space. δ is the wire diameter equals to 1.5 mm, z is the distance from the coil center that the field strength is measured there. Inner (r_1) and outer (r_2) radius of the coil was 23 and 83 mm, respectively. The resistance of each coil was 1.5 Ohm.

Separation between the two coils in parallel state was 6 cm. The measurements showed that there is good agreement between computational and measured magnetic field strength. In order to increase parallel

magnetic field strength, we inserted ferrite cores into the coils. The dimension of the ferrite core was $26\times 26\times 80m^3$.

Finally, the magnetic field strength applied to plasma jet, was at focused point for optical intensity measurement, about 0.2 Tesla, in the case of the maximum specified current of power supply, I=18 A. The focused point for intensity measurement by spectroscopy and photography methods was shown in fig1a. In this point, the width of jet is about 3mm.

To record the emission of the jet, we employed UV-IR compact wide range 190-1100 nm spectrometer (S-100, Solar-Laser system). To capture the photograph of the jet and process the intensity profile, a digital camera (SONY PSC-HX-20 18.1 Megapixel) was used.

During optical emission spectroscopy, argon emission spectra was measured at vertical position to the jet direction and to the magnetic field direction. The relationship between the emission intensity, I_p, and the optical radiation intensity, I, is estimated by the following expression

$$I \propto \int I_p d\lambda \qquad (5)$$

where, λ is the wavelength.

After running the jet, the temperature of plasma jet increases gradually. For example: it raises from room temperature to 50 $^{\circ}$C in 20 minutes. it leads to the plasma number density increase. The atmospheric pressure plasma jet irradiance increases gradually due to gas temperature increase. Temperature increment takes place both with and without magnetic field. To decompose gradually increment of temperature effect from that of the magnetic field, spectroscopy was taken in discrete and continuous forms. In discrete form, by spectroscopy, argon spectra emission was collected with optical probe, 60 seconds after ignition. Then the jet was turned off for several minutes for cooling. Then it was generated again and its emission was recorded in the presence of the magnetic field. This method guarantied the same temperature for plasma measurements.

In the continuous form, the plasma jet wasn't turned off during the measurements; instead, the external magnetic field was switched off in time intervals. Plasma jet was generated and after 10 seconds, by spectroscopy, the jet emission was collected, then after 60 seconds, its emission was recorded again. In the next process, magnetic field was applied and after 60 seconds, the jet emission spectra was recorded. Then its emission was collected after 60 seconds in magnetic field-free and in final process, magnetic field was applied again and plasma jet emission was recorded. Both continuous and discrete forms were carried out by photography in conjunction with optical emission spectroscopy.

EXPERIMENTAL RESULTS

Application of the direct current external magnetic field has effect on the non-thermal plasma jet radiation. In the discrete case, Figure 4 shows comparison between argon emission spectra in the presence and absence of the external magnetic field in the parallel state. As shown in Figure 4, the emission intensity increased at all wavelengths

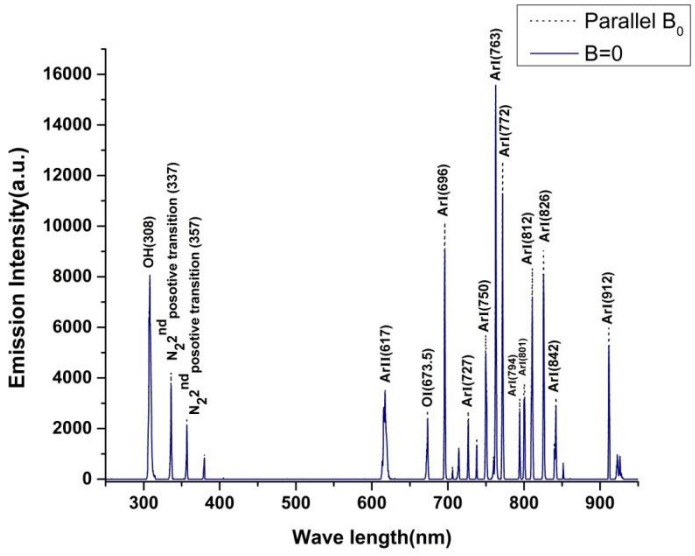

Figure4. Comparison between argon emission spectra in the presence and absence of the parallel external magnetic field

The variation of the optical radiation intensity obtained from imaging technique and spectroscopy method, in the discrete form, was shown in Figure 5. In the presences of the parallel external magnetic field, the optical radiation intensity of the jet increased.

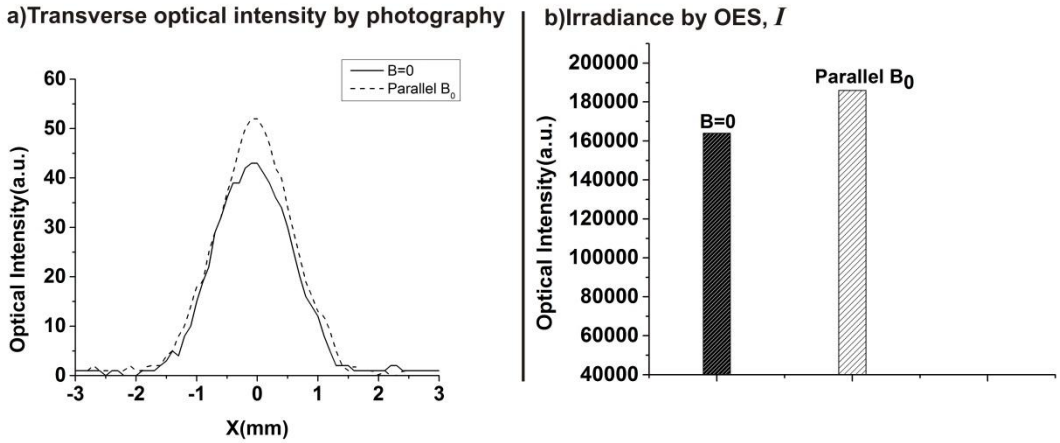

Figure5. The variation of the optical radiation intensity in the presence of the parallel magnetic fields, by (a) imaging technique and (b) Spectroscopy method

As mentioned, image analysis software was utilized to obtain the optical radiation in transverse and axial directions with respect to the flow velocity. Figure 6 shows parallel magnetic field effect on the optical radiation intensity distribution along with the jet flow in the discrete form.

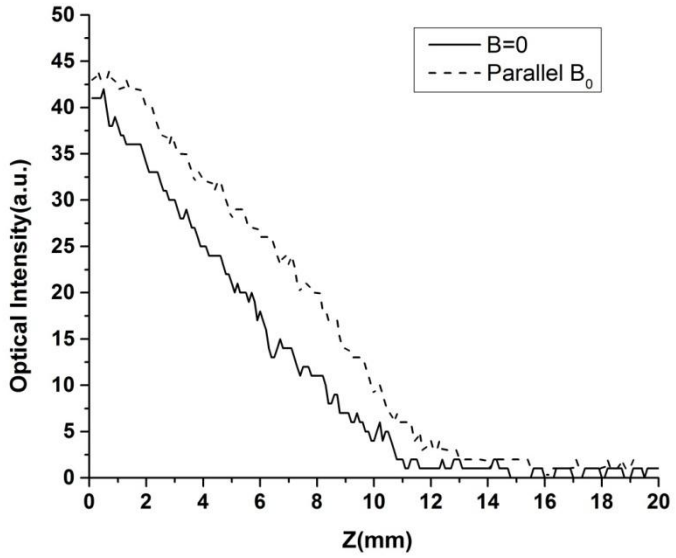

Figure6. The variation of the optical radiation intensity in the presence of the parallel magnetic field, along the jet flow direction, captured by the camera

In presence of parallel magnetic field, optical intensity in direction of the centerline axis, increased. These results indicate that the distribution of optical radiation intensity in this direction is in good agreement with vertical direction.

In the continuous form (without turning off the jet), the external magnetic field is applied in two time intervals. Figure 7 shows the optical radiation intensity that was recorded by the spectroscopy method in the case of parallel magnetic field. As can be observed, by applying the external parallel magnetic field, the optical radiation intensity increased while in field-free case, it was increased due to gradually increment of the plasma jet temperature.

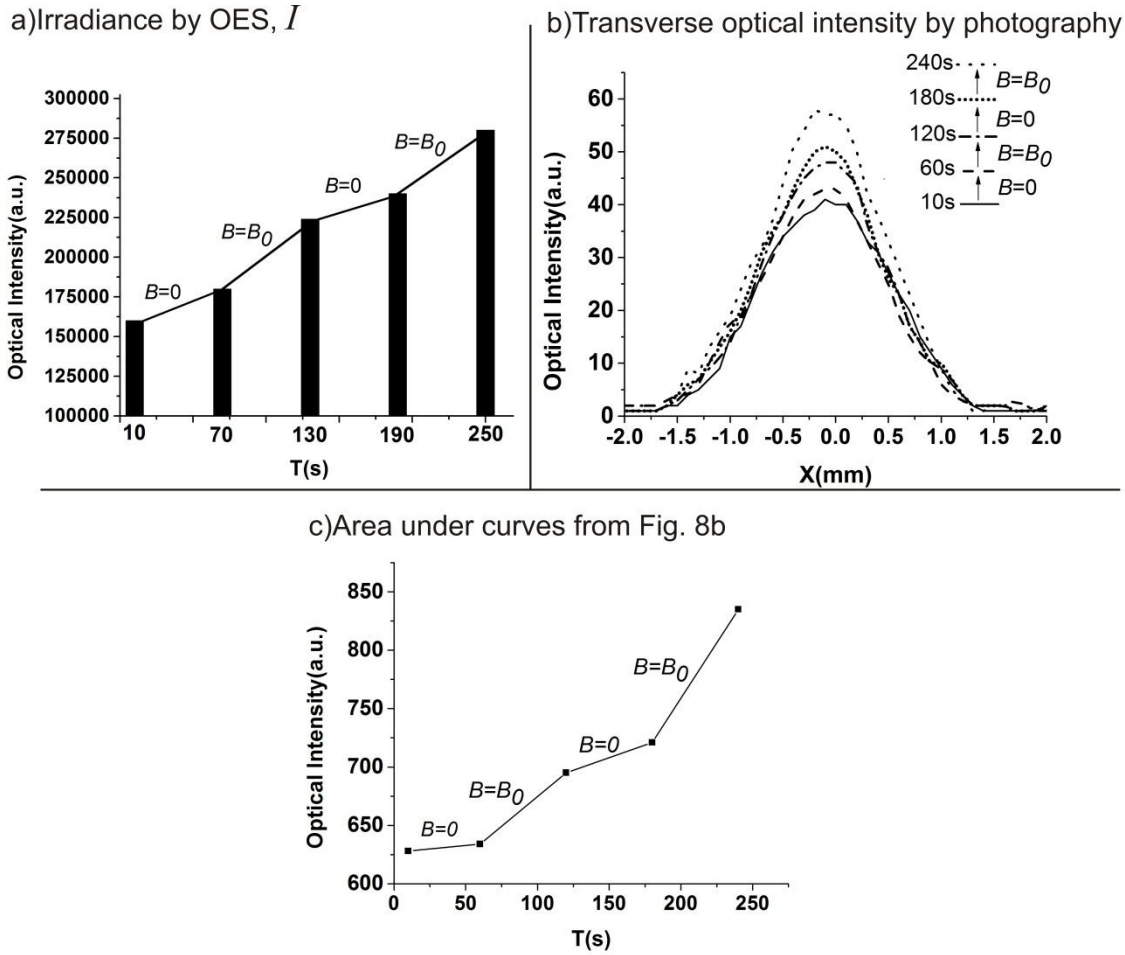

Figure7. The variation of the optical radiation intensity in the presence of the parallel magnetic field, in the continuous form by (a) Spectroscopy method and (b) Imaging technique

DISCUSSIONS AND ANALYTICAL MODELS

In this paper, the optical emission spectroscopy and the imaging technique were utilized to quantify the plasma jet behavior under the external magnetic field. The distribution of the optical radiation intensity obtained from raw image files, agree well with that of the spectral intensity in the continuous and discrete situations.

Parallel field

In the parallel state, the jet assembly inserted between the Helmholtz coils. In this state, as shown in Fig. 1c, both magnetic field and the plasma jet axis are in Z-direction. Figure 8 depicts the flow velocity vectors of the plasma jet in three distinct zones. Zone 1 illustrates the space between the electrodes where the plasma initiates, zone 2 depicts the nozzle orifice where it is contracted and zone 3 shows effluent plasma jet with negligible excitation electric field. One can use single fluid MHD equation to investigate the plasma jet. In zones 1 and 3, the flow velocity is parallel to the external magnetic field, therefore the term $\vec{V}\times\vec{B}=0$ in MHD Ohm's law. In steady state, in zone 2, MHD Ohm's law can be written as

$$\vec{E}+\vec{V}\times\vec{B}=\frac{\vec{J}}{\sigma} \qquad (6)$$

Where $\vec{E}$, is induced electrostatic electric field, $\vec{V}$ describes the plasma jet flow velocity, $\vec{B}$ is the external magnetic field, $\vec{J}$ is the induced current outside the electrodes and σ is the plasma conductivity.

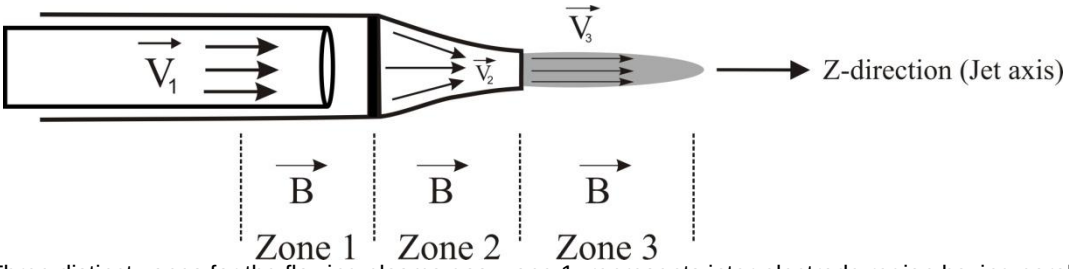

Figure 8. Three distinct zones for the flowing plasma gas: zone 1, represents inter-electrode region having parallel velocity with $\vec{B}$; zone 2, represents nozzle orifice with radial velocity and zone 3, depicts effluent plasma jet having parallel velocity with $\vec{B}$

Regarding to the plasma jet assembly that illustrated in Fig. 1a, the nozzle was contracted led to radial flow velocity during exiting the nozzle. Then, the flow velocity has two components at the nozzle region (zone 2), parallel and perpendicular to the external magnetic field

$$\vec{V} = \vec{V_r} + \vec{V_z} \quad (7)$$

Where, $\vec{V_r}$ is the radial flow and $\vec{V_z}$ is the flow velocity of the plasma jet along with the external magnetic field. It can be seen that the radial flow induces an azimuthally plasma current density J_θ during exiting the nozzle orifice,

$$J_\theta = \sigma(V_r B_z + E_\theta) \quad (8)$$

This process reduces plasma loss to the walls led to enhancing plasma number density and plasma jet irradiance as well. It is seen that the induced current density is proportional to the jet flow velocity and external magnetic field strength.

Another reason for increasing plasma number density can be addressed to the previous works on the magneto-active plasmas (Sohbatzadeh et al., 2004; Sohbatzadeh and Latifi, 2004). As illustrated in Figs. 1(a) and 8, the electric field between the electrodes has two components at zone 1, parallel and perpendicular to the external magnetic field that can be described by

$$\vec{E}(t) = \vec{E_r}(t) + \vec{E_z}(t) \quad (9)$$

Our previous works showed that the transverse electric field $\vec{E_r}$ between the electrodes increases in a magneto-active plasma. This process can lead to further ionization and produces more charged particles, i.e., increases plasma number density as well.

CONCLUSIONS

An experimental study was carried out to clarify non-thermal atmospheric pressure plasma jet behavior under the application of the external magnetic field, in the parallel form. It was concluded that by applying external magnetic field parallel to the jet axis, irradiance of the plasma jet can be affected and changed considerably. It was confirmed that in the presence of a magnetic field parallel to the centerline axis of the jet, the optical intensity increases. The increase of light intensity was attributed to plasma loss decrease by magnetic force in zone 2. The plasma considered here is collisional; therefore the mobility and diffusion coefficient could not be affected by the external magnetic field, substantially. As a result, the related mobility and conductivity tensors are to be scalar coefficients for magneto-active atmospheric pressure plasma jet in the presence of external magnetic field. This investigation confirmed that the magneto-active atmospheric pressure plasma description is not the same as that of low pressure. It was concluded that the plasma fluid velocity is responsible for changes in magneto-active plasma jet irradiance via magnetic force $\vec{V} \times \vec{B}$, where $\vec{V}$ is the flow velocity vector. The results of this work can be used to control the plasma jet number density.

REFERENCES

Koike K, Ono N, Watanable Y, Musha K. 2004. Measurement on the excitation temperature of argon plasma jet under strong magnetic field. Vacuum. 73: 353-358.

Koike K, Ono N. 2008. Light intensity analysis of plasma jet constriction with applied magnetic field. Vacuum. 83: 25–28.

Krall NA, Trivelpiece AW. 1973. Principles of Plasma Physics. McGraw-Hill, New York.

Lu X, Jiang Z, Xiong Q, Tang Z, Hu X, Pan YK. 2008. An 11cm long atmospheric pressure cold plasma plume for applications of plasma medicine. Appl. Phys. Lett. Vol. 92.

Lu X, Laroussi M, Puech V. 2005. On atmospheric-pressure non-equilibrium plasma jets and plasma bullets. Plasma Sources Sci. Technol. Vol. 21.
Ono N, Musha K, Koike K. 2006. A simple diagnostic method for plasma jet in strong magnetic field. Vacuum. 80: 1179-1184.
Ono N, Otomo Y, Koike K. 2007. Behavior of Underexpanded Plasma Jet in Strong Magnetic Field. J. Visualization. 10: 237-244.
Raizer YuP. 1997. Gas Discharge Physics. Springer, Verlag Berlin Heidelberg.
Schutze A, Jeong JY, Babayan SE, Park J, Selwyn GS, Hicks RF. 1998. The atmospheric-pressure plasma jet: a review and comparison to other plasma sources. Plasma Science, IEEE Transactions on. 26: 1685-1694.
Sohbatzadeh F, Latifi H. 2004. Quasilinear collisionless electron heating in a weakly magnetized inductively coupled plasma. J. Plasma Phys. 70: 671-680.
Sohbatzadeh F, Tavassoli H, Latifi H. 2004. The influence of an external magnetic field on a radio frequency excited CO2 laser. Phys. Plasmas. 11 3904-3910.
Tendero C, Tixier C, Tristant P, Desmaison J, Leprince P. 2006. Atmospheric pressure plasmas: A review. Spectrochimica Acta Part B: Atomic Spectroscopy. 61: 2-30.
Walsh JL, Iza F, Janson NB, Law VJ, Kong MG. 2010. Three distinct modes in a cold atmospheric pressure plasma jet. J. Phys. D: Appl. Phys. Vol. 43.